

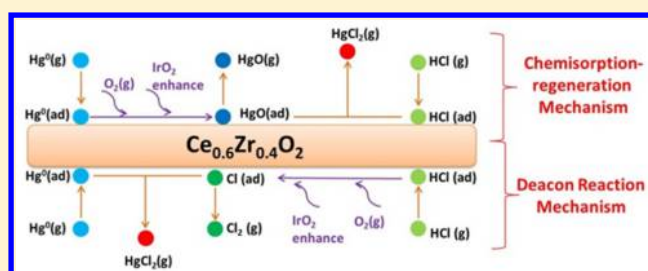
Novel Effective Catalyst for Elemental Mercury Removal from Coal-Fired Flue Gas and the Mechanism Investigation

Wanmiao Chen, Yang Pei, Wenjun Huang, Zan Qu, Xiaofang Hu, and Naiqiang Yan*

School of Environmental Science and Engineering, Shanghai Jiao Tong University, 800 Dong Chuan Road, Shanghai, 200240 PR China

S Supporting Information

ABSTRACT: Mercury pollution from coal-fired power plants has drawn attention worldwide. To achieve efficient catalytic oxidation of Hg^0 at both high and low temperatures, we prepared and tested novel IrO_2 modified Ce–Zr solid solution catalysts under various conditions. It was found that the $\text{IrO}_2/\text{Ce}_{0.6}\text{Zr}_{0.4}\text{O}_2$ catalyst, which was prepared using the polyvinylpyrrolidone-assisted sol–gel method, displayed significantly higher catalytic activity for Hg^0 oxidation. The mechanism of Hg^0 removal over $\text{IrO}_2/\text{Ce}_{0.6}\text{Zr}_{0.4}\text{O}_2$ was studied using various methods, and the Hg^0 oxidation reaction was found to follow two possible pathways. For the new chemisorption–regeneration mechanism proposed in this study, the adsorbed Hg^0 was first oxidized with surface chemisorbed oxygen species to form HgO ; the HgO could desorb from the surface of catalysts by itself or react with adsorbed HCl to be release in the form of gaseous HgCl_2 . O_2 is indispensable for the chemisorption process, and the doping of IrO_2 could facilitate the chemisorption process. In addition, the Deacon reaction mechanism was also feasible for Hg^0 oxidation: this reaction would involve first oxidizing the adsorbed HCl to active Cl species, after which the Hg^0 could react with Cl to form HgCl_2 . Additionally, doping IrO_2 could significantly improve the Cl yield process. In summary, the novel IrO_2 modified catalyst displayed excellent catalytic activity for elemental mercury oxidation, and the proposed reaction mechanisms were determined reasonably.



INTRODUCTION

Mercury is a heavy metal pollutant with high levels of toxicity, bioaccumulation, and persistence that has caused worldwide concern.¹ The *Minamata Convention on Mercury* regarding mercury pollution was signed by many governments in 2013, which pressured major mercury emitters such as China and the United States to reduce mercury emissions.^{2,3} Coal-fired power plants are the primary sources of anthropogenic mercury pollution to the atmosphere because of high levels of coal consumption. Some researches proposed that mercury from coal-fired boilers contributed approximately 40% of the total mercury emissions in China.^{4,5} Mercury can exist in coal-fired flue gas in three different forms: elemental mercury (Hg^0), gaseous oxidized mercury (Hg^{2+}), and particulate-bound mercury (Hg^p). The distribution of these forms mainly depends on the chlorine content of the coal and the combustion conditions.⁶ Most oxidized and particulate-bound mercury can be easily removed from the exhaust with typical air-pollution-control devices (APCDs). However, Hg^0 is highly volatile and insoluble and is the dominant mercury species that escapes into the atmosphere from coal-fired power plants. Therefore, the catalytic oxidation of Hg^0 to Hg^{2+} (which can be dissolved in water and captured by WFGD under certain conditions) with HCl from flue gas is an economical and feasible method for achieving greater mercury removal efficiency with existing APCDs.^{6–10} For example, the catalysts involved in the process

of selective catalytic reduction (SCR) of NO_x , which usually occurs at 300–400 °C,¹¹ have been investigated as potential Hg^0 conversion catalysts when sufficient HCl is present in the flue gas.^{6,12} However, the presence of ammonia (NH_3), which is used as an SCR reductant, can significantly inhibit Hg^0 oxidation over conventional SCR catalysts.^{12,13} Therefore, it is reasonable to equip Hg^0 oxidation catalysts at the tail section of the SCR unit, where the NH_3 concentration is lower. In addition, the low-temperature SCR (approximately 150 °C) technique has become more popular in recent years and has a tendency for future industrial applications.¹⁴ Therefore, it is important to develop a new catalyst that could convert elemental mercury significantly at lower temperatures and thus be compatible with low-temperature SCR catalysts.

Many studies have proposed that the catalytic oxidation of Hg^0 to Hg^{2+} over some catalysts with presence of HCl could be explained through the Deacon reaction pathway, in which HCl is converted to Cl_2 or Cl atoms by oxygen.^{15–18} IrO_2 has proven to be an active catalyst for the Deacon reaction, effectively converting HCl to Cl_2 .^{19,20} Thus, IrO_2 is expected to be a promising catalyst component for Hg^0 conversion in the

Received: November 11, 2015

Revised: January 23, 2016

Accepted: January 27, 2016

Published: January 27, 2016

presence of HCl. A solid solution of ceria (Ce) and zirconia (Zr) with cubic fluorite phase (Ce/Zr > 1:1) has been used as the catalyst carrier in recent studies because of its outstanding oxygen storage capacity and unique redox properties.^{11,21–23} In previous studies, catalysts for elemental mercury oxidation were developed from SCR catalysts,²⁴ and Ce–Zr solid-solution-supported metal oxide catalysts exhibited significant catalytic activity for low-temperature-selective catalytic reduction of NO_x from coal-fired flue gas.²³ Other previous studies have reported that Ce–Zr supported catalysts display excellent catalytic oxidation ability for the ammonia slipping from SCR units, which would also mitigate the negative effects of NH₃ on elemental mercury oxidation.²⁵ Therefore, the Ce–Zr solid solution is a promising catalyst for Hg⁰ oxidation that would be compatible with SCR units at both high and low temperatures. Although Ir has been used as mercury-removal sorbent,¹⁴ the catalytic activity of the IrO₂ modified Ce–Zr complex for mercury oxidation is still unclear. In addition, the interaction between IrO₂ and the Ce–Zr supporter has not been studied previously. Mechanisms including the Mars–Maessen mechanism, the Eley–Rideal mechanism, and the Langmuir–Hinshelwood mechanism^{6,26} have been proposed for mercury oxidation over various catalysts.¹⁷ However, the mechanism of mercury removal over IrO₂ modified catalyst is unclear. In particular, there is still no consensus regarding the role of Cl in the process of elemental mercury oxidation. Thus, we focus on the mechanism of mercury oxidation in this study.

Because Ir is a noble metal and is thus more expensive than most transition metals, the IrO₂ content was set a very low level (0.2%). To maintain catalytic performance despite the low Ir concentration, we used the sol–gel method with polyvinylpyrrolidone (PVP) to enhance the dispersion of IrO₂ on the catalyst surface. We evaluated the efficiency of elemental mercury removal and adsorption behavior over various modified catalysts. In addition, we evaluated the possible catalytic mechanisms of elemental mercury using techniques such as H₂ temperature-programmed reduction (TPR), Hg temperature-programmed desorption (TPD), and Cl₂ yield. We focus our discussion on the effects of IrO₂ and Cl in the oxidation process.

EXPERIMENTAL SECTION

Materials and Catalyst Preparation. The IrO₂ doping catalysts were synthesized according to a method reported in literature.²⁷ First, 0.2 g polyvinylpyrrolidone (Mw = 58 000) and quantitative iridium acetate were dissolved in 30 mL of ethanol, and the mixture was refluxed at 100 °C for 3 h. After this, the Ir colloidal solution was added to Ce_xZr_{1–x}O₂ (see the Supporting Information), and the mixture was dried at 60 °C with electromagnetic stirring. Calcination was achieved by increasing the temperature from room temperature to 400 °C at a 1 °C/min ramping rate, after which the solution was heated at 400 °C for 5 h in air. The catalysts were labeled as IrO₂/Ce_xZr_{1–x}O₂ (PVP). IrO₂/Ce_xZr_{1–x}O₂ was prepared with the wet impregnation method.²⁸ The Ir oxide content of Ce_xZr_{1–x}O₂ was set at 0.2 wt % for all catalysts.

Catalyst Characterization. X-ray photoelectron spectroscopy (XPS) measurements were taken with an AXIS UltraDLD (Shimadzu–Kratos) spectrometer with Al Kα as the excitation source. The C 1s line at 284.8 eV was used as a reference for the binding-energy calibration. The H₂ temperature program reduction curves were determined using a chemisorption analyzer (2920, AutoChem II, Micromeritics). The H₂ flow

rate was 50 cm³/min, and the temperature ramp rate was 10 °C/min.

Catalytic Activity Measurement. The Hg⁰ adsorption and catalytic oxidation experiments over catalysts were performed in a fixed-bed quartz reactor; the experimental system is shown in Figure S1. The catalysts powder was placed in the reactor with quartz wool under atmospheric pressure, and the reactor was heated by a vertical electrical furnace. The feed gases were adjusted by mass-flow controllers and introduced into the reactor with a total flow rate of 500 mL/min. The gas with stable elemental mercury concentration from a Hg⁰ permeation tube flowed through the blank tube and the reactor tube. The mercury concentration was monitored by a Lumex 915+ or Tekran 3300 mercury analyzer. The Tekran 3300 systems were programmed to measure Hg^T and Hg⁰ semicontinuously over a 2.5 min collection–analysis cycle. The reported Hg²⁺ fraction was calculated as the difference between sequentially measured Hg^T and Hg⁰ concentrations.

For the Hg⁰ adsorption experiment, the Hg⁰ flow first passed through the blank tube to provide an original Hg⁰ signal. The Hg⁰ concentration for the adsorption experiment was ranged from 370 to 1500 ng/L for the different experiments. We used these high concentrations for two reasons. First, the Hg⁰ adsorption capacity of our catalysts is very high, so if a normal mercury concentration was used, it would take long time to reach equilibrium. High mercury concentration could shorten the adsorption time. Many previous studies have also used high mercury concentration.^{29,30} Second, high mercury concentration can minimize the relative error due to continuous data acquisition in the tests. For the results obtained from Tekran 3300 mercury analyzer, the mercury concentration was approximately 370 ng/L due to the test limit. After the Hg⁰ concentration had stabilized, the Hg⁰ concentration in the outlet was measured as [Hg⁰]₁, and then the gas was switched to the reactor tube to begin Hg⁰ adsorption. For the Hg⁰ catalytic oxidation experiment with HCl and O₂, the flow containing mercury was first passed through the catalysts to undergo adsorption. Next, HCl or other gases were added to the gas, and the Hg⁰ concentration in the outlet was measured as [Hg⁰]₂ until the reaction attained equilibrium (stable for long time). The Hg⁰ oxidation efficiency (*E*_{oxi}) over the catalysts was quantified by the following equation:

$$E_{\text{oxi}} (\%) = \frac{[\text{Hg}^0]_1 - [\text{Hg}^0]_2}{[\text{Hg}^0]_1} \times 100\%$$

Hg-TPD was conducted using 30 mg of the catalyst in a quartz reactor. First, the Hg⁰ adsorption achieved by passing a gas mixture containing approximately 1090 ng/L Hg⁰ with O₂/N₂ or N₂ as the balance gas through the reactor tube at 150 °C for 90 min with a total flow rate of 500 mL/min; next, the reactor tube was purged with N₂ for 30 min. Desorption measurements were performed from 150 to 500 °C at a heating rate of 5 °C/min under a N₂ atmosphere of 500 mL/min. An online mercury analyzer continuously recorded the desorbed concentration of Hg⁰.

Finally, the mechanism of Hg⁰ oxidation was evaluated using Deacon reaction evaluation units (with chlorine yield as the marker). The Cl₂ concentration was monitored using a UV/vis spectrometer (BWTEK BRC642E) with a photocell constructed to have an optical length of 80 cm.

RESULTS AND DISCUSSION

Catalytic Activity. The Figure 1 shows the catalytic oxidation efficiencies over catalysts under various conditions;

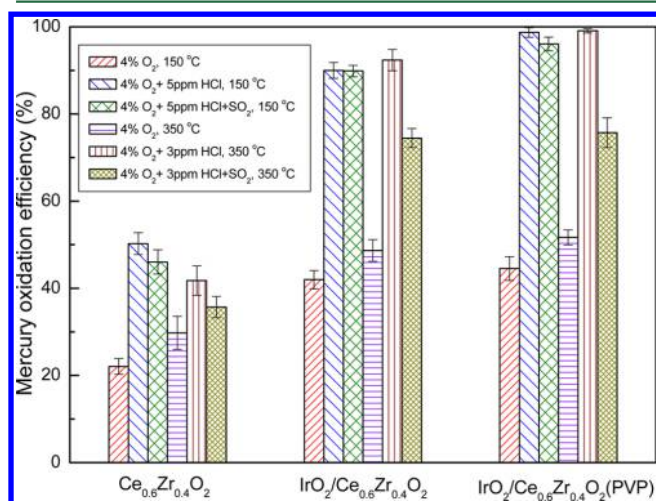


Figure 1. Catalytic oxidation of Hg⁰ over various catalysts and different condition at 350 and 150 °C. Reaction conditions: 500 ppm of SO₂; O₂, 4 vol %; N₂ as carrier; flow rate, 500 mL/min; catalyst weight, 30 mg. The space velocity (SV) was approximately 7.6×10^5 h⁻¹.

preliminary tests showed that Ce_{0.6}Zr_{0.4}O₂ supported catalysts displayed superior catalytic activity (Figure S2). The Hg⁰ oxidation efficiency over Ce_{0.6}Zr_{0.4}O₂ was 22% when there was only 4% O₂ in the gas at 150 °C. The mercury-removal efficiencies over IrO₂ modified catalysts increased to approximately 41% and 44% in the presence of O₂ for IrO₂/Ce_{0.6}Zr_{0.4}O₂ and IrO₂/Ce_{0.6}Zr_{0.4}O₂ (PVP), respectively, which indicated that doping with only 0.2% IrO₂ could significantly facilitate Hg⁰ conversion even without HCl. When HCl was introduced into the gas, mercury removal efficiencies were enhanced significantly over all three catalysts. For example, the mercury removal efficiency over IrO₂/Ce_{0.6}Zr_{0.4}O₂ increased from 41% to 90% in the presence of 3 ppm of HCl at 350 °C. The synthesis method also had an effect on the catalytic activity. The Hg⁰ oxidation efficiency over IrO₂/Ce_{0.6}Zr_{0.4}O₂ (PVP) increased to approximately 97% at 150 °C. We propose that PVP might promote IrO₂ dispersion over the carrier, similar to results in other studies, and the catalytic activity was slightly enhanced in consequence.²⁷ We also tested the effects of SO₂ on Hg⁰ oxidation. Results showed that SO₂ had a different influence on all three catalysts at high and low temperatures. We note that mercury concentrations decreased during addition of SO₂ at both high and low temperatures (Figure S3). Some previous studies have proposed that SO₂ could be transferred to SO₃ over some catalysts and that SO₃ could improve the adsorption of Hg⁰ to the catalysts.³¹ After the adsorption saturation was reached, the Hg⁰ concentration in the outlet began to increase (Figure S3), and SO₂ then displayed inhibition on Hg⁰ removal. At high temperatures, 500 ppm of SO₂ could obviously inhibit mercury removal over all three catalysts. For example, the mercury oxidation of the IrO₂/Ce_{0.6}Zr_{0.4}O₂ (PVP) catalyst decreased from 99% to 75% in the presence of SO₂ at 350 °C. However, the catalysts displayed excellent tolerance for SO₂ poisoning at lower temperatures, at which SO₂ had negligible effects on mercury removal over all three catalysts. In addition, the Hg⁰ oxidation efficiency of

IrO₂/Ce_{0.6}Zr_{0.4}O₂ (PVP) was greater than 90% in the simulated coal-fired flue gas (including NO, NH₃, SO₂, H₂O, O₂, and N₂) over a long experimental duration at both high and low temperatures (Figure S4 and S5). The results showed that catalysts had excellent durability for the complex components in the flue gas.

Adsorption Experiment. Adsorption generally plays a significant role in catalytic reactions. Therefore, to determine the catalytic mechanism of mercury oxidation over the IrO₂ modified catalysts, we evaluated the adsorption of Hg⁰ under various conditions (Figure 2). First, Hg⁰ adsorption was

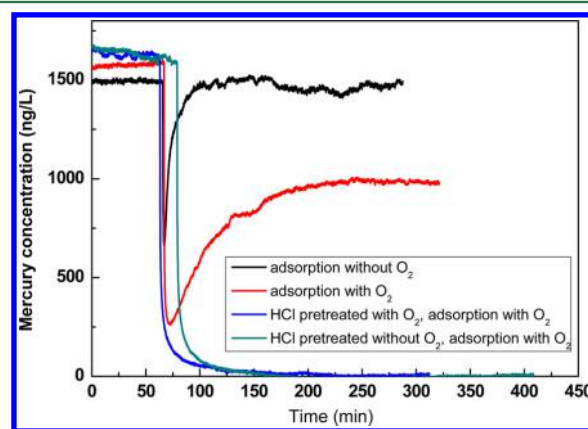


Figure 2. Adsorption breakthrough curves of Hg⁰ over the IrO₂/Ce_{0.6}Zr_{0.4}O₂ (PVP) catalysts under different conditions. Reaction conditions: 4 vol % O₂; N₂ as carrier; flow rate, 500 mL/min; catalyst weight, 30 mg. The space velocity was approximately 7.6×10^5 h⁻¹. The temperature was 350 °C.

performed over the IrO₂/Ce_{0.6}Zr_{0.4}O₂ catalyst in the absence of O₂, and adsorption equilibrium was reached quickly within 30 min. After adsorption saturation was reached, the Hg⁰ concentration recovered to initial levels, such that Hg⁰ could no longer be converted over the catalyst in the absence of O₂. However, the breakthrough curve was very different in the presence of O₂, the adsorption capacity was much larger with O₂ present and the reaction took approximately 165 min to reach adsorption saturation. These results indicate that the adsorption process of Hg⁰ over the IrO₂/Ce_{0.6}Zr_{0.4}O₂ catalyst is likely a chemisorption process, and that O₂ is indispensable for this process. The final detected concentration for Hg⁰ was approximately 60% of the initial level, which suggests that Hg⁰ can be oxidized over the IrO₂ modified catalyst in the absence of HCl. This agrees with the results shown in Figure 1.

Halogens can strongly affect mercury removal. To clarify the effect of gaseous HCl, we also performed the Hg⁰ adsorption experiment over a IrO₂/Ce_{0.6}Zr_{0.4}O₂ catalyst pretreated with HCl. The IrO₂ modified catalyst was pretreated with 10 ppm of HCl and 4% O₂ with N₂ carrier at 350 °C for 4 h, after which it was purged with N₂ for 1 h. Next, the Hg⁰ adsorption experiment was carried out, and the adsorption Hg curve is shown in Figure 2. The result shows that the adsorption capacity of the catalyst was significantly improved by HCl treatment, and the removal efficiency of elemental mercury was higher than 99%, even after interacting with Hg⁰ for 300 min. To identify the interaction between HCl and O₂ and evaluate the role of O₂, we performed another Hg⁰ adsorption experiment over the catalyst. The catalyst was pretreated under 10 ppm of HCl without O₂ for 4 h, after which it was purged with N₂ for 1 h.

The resulting adsorption curve was similar to the curve from the treatment with HCl and O₂, showing that HCl can have an effect on mercury removal in the absence of O₂. Additionally, this result suggests that HCl and O₂ might not interact during the reaction.

Hg-TPD. After the mercury adsorption experiments, we used the Hg-TPD technique to identify the mercury captured on the IrO₂/Ce_{0.6}Zr_{0.4}O₂ catalysts, and the results are shown in Figure 3. After the catalyst adsorbed Hg⁰ in 4% O₂/N₂ atmosphere,

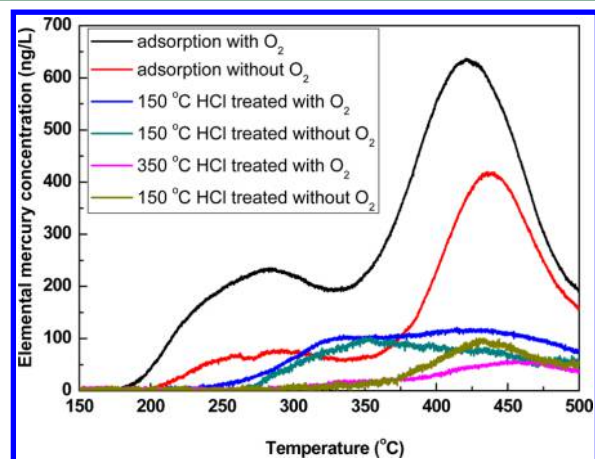


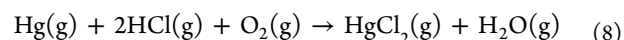
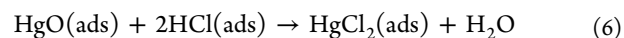
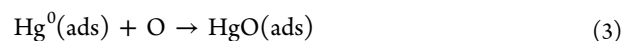
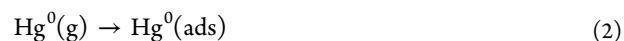
Figure 3. Temperature-programmed-desorption of Hg over the IrO₂/Ce_{0.6}Zr_{0.4}O₂ (PVP) catalysts under different conditions.

two main desorption peaks are present at approximately 284 and 425 °C. According to some literature, two desorption peaks centered at approximately 110 and 260 °C can be observed over many catalysts during Hg-TPD experiment, and these correspond to the decomposition of weakly adsorptive species and strongly bound species, respectively.³² Because the adsorption experiment in this research was performed at 150 °C, it is reasonable that we cannot detect desorption peaks below 150 °C. The peak at 284 °C is close in value to the peak at approximately 260 °C shown by previous studies, so we suggest that it may reflect the desorption of strongly bound, physically adsorbed Hg⁰. The desorption peak at higher temperatures, then, likely corresponds to the decomposition of HgO.³³ The fact that the peak area at 425 °C is much larger than the peak area at 284 °C indicates that the majority of the mercury species existed as HgO and chemisorption was the dominant mode of Hg⁰ adsorption on the IrO₂ modified catalyst. While, the intensities of the desorption peaks were much weaker over the catalyst that adsorbing Hg⁰ in a pure N₂ atmosphere. The desorption peak of HgO is still observed, possibly because Hg⁰ could still be chemically adsorbed and converted to HgO due to the outstanding oxygen storage capacity of the Ce_{0.6}Zr_{0.4}O₂ carrier.

To evaluate the effect of HCl on mercury adsorption, we pretreated the catalyst with HCl and O₂/N₂ atmosphere at 150 and 350 °C, respectively, before Hg⁰ adsorption, and the results are also given in Figure 3. A broad desorption shoulder is present from 250 °C over the catalyst pretreated with HCl under an 4% O₂/N₂ at 150 °C. Meanwhile, a desorption peak is centered at 450 °C for the catalyst pretreated under HCl with 4% O₂ at 350 °C. The intensities of the mercury desorption peaks over the catalyst after HCl treatment were much weaker than the fresh catalysts, which meant the amount of mercury adsorbed over the catalyst became much less because of the

HCl treatment. Some studies have shown that the thermal decomposition of HgCl₂ phase occurs at low temperatures ranging from 70 to 220 °C (with a maximum at 120 °C).³⁴ Our results did not show any such desorption peaks over the HCl-pretreated catalysts, indicating that none of the HgCl₂ species existed over the surface of the HCl-pretreated catalysts, even after Hg⁰ adsorption. We also treated the catalyst with HCl in N₂ atmosphere at 350 °C before Hg⁰ adsorption. The resulting desorption profile was similar, and no obvious desorption peak was detected for the catalyst pretreated with HCl in N₂. This result suggests that HCl can affect the reaction in the absence of O₂, which supports the results shown in Figure 2.

The results in Figures 2 and 3 seem “contradictory”. Figure 2 shows that HCl treatment with or without O₂ can significantly improve the apparent adsorption capacity of Hg⁰ over the catalyst. In contrast, Figure 3 shows that the amount of desorption of adsorbed mercury over the HCl pretreated catalyst was much less than that the amount from fresh catalyst. To explain these “contradictory” situation, we propose a new mechanism called the chemisorption–regeneration mechanism. First, elemental mercury is adsorbed to the surface of the catalyst, and the adsorbed Hg⁰ is oxidized with surface-chemisorbed oxygen species to form HgO (see reactions 2–3 below). The portion of formed HgO can desorb from the catalyst’s surface in the absence of HCl, which would regenerate active adsorption sites (reaction 4). Some studies have proposed that O₂ can be dissociated over IrO₂ catalyst (reaction 1),³⁵ which could replenish the consumption of active oxygen. This could explain why elemental mercury could be oxidized in the presence of O₂ alone in Figure 1. When HCl exists in gas, it can adsorb to the catalyst surface and then react with formed HgO to HgCl₂ (reactions 5–7). HgCl₂ is much easier to be released as a gas from the surface of the catalyst.³⁶ In this reaction pathway, HCl could affect the mercury adsorption property of the catalyst even in the absence of O₂. When the HCl treatment and Hg⁰ adsorption with O₂ were divided factitiously into two separate processes, as in the experiments shown in Figures 2 and 3, they demonstrated the chemisorption process for reactant and the regeneration process for the catalyst. When Hg⁰, O₂, and HCl coexisted in the experiment as shown in Figure 1 (and in real coal-fired flue gas), the chemisorption process and regeneration process by HCl could proceed simultaneously. The apparent experimental result was that Hg⁰ is converted into HgCl₂ continuously. The overall reaction could be considered to be catalytic oxidation, as in reaction 8.



Verification of the Proposed Mechanism. To verify the mechanism proposed above, we employed a Tekran mercury

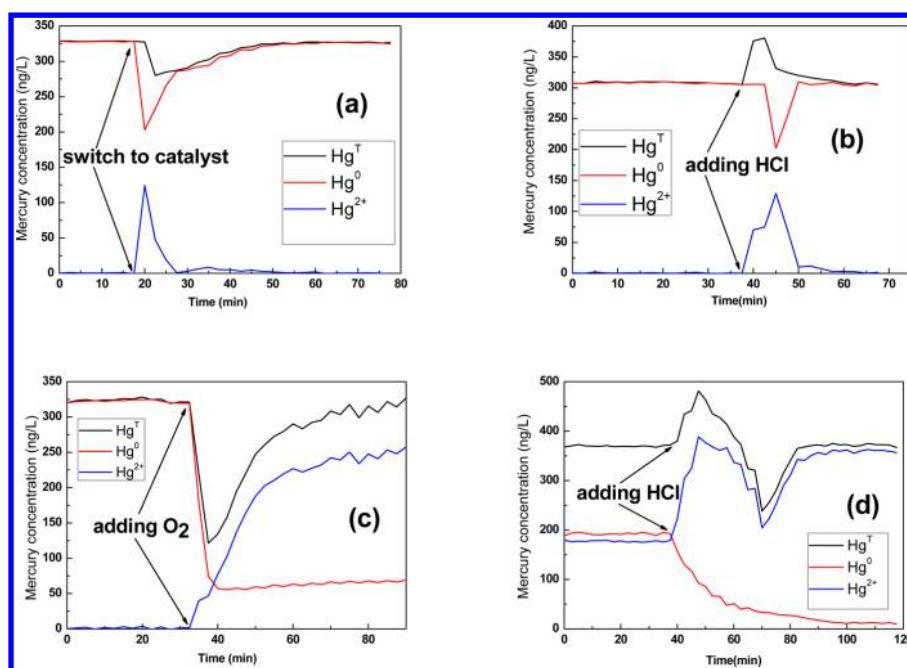


Figure 4. Mercury removal experiments on the Tekran mercury analyzer. Reaction conditions: 10 ppm of HCl; O₂, 4 vol %; N₂ as carrier; flow rate, 500 mL/min; catalyst weight, 30 mg. The space velocity (SV) was approximately $7.6 \times 10^5 \text{ h}^{-1}$. The temperature was 350 °C. (a) N₂ balance; (b) N₂ balance, adding HCl; (c) N₂ balance, adding 4% O₂; (d) N₂ balance, 4% O₂, adding HCl.

analyzer that could simultaneously monitor total mercury (Hg^T) and elemental mercury (Hg⁰) in gas to perform mercury oxidation experiment. First, N₂ gas with Hg⁰ passed through the IrO₂/Ce_{0.6}Zr_{0.4}O₂ (PVP) catalyst, and the results are shown in Figure 4a. Although no O₂ was present in the gas, some Hg²⁺ in the initial stage of adsorption was detected in the exhaust. This could be explained by the fact that adsorbed Hg⁰ was oxidized by active oxygen species from the Ce–Zr solid solution due to its outstanding oxygen storage capacity, which will be discussed later. After adsorption equilibrium was reached, HCl was introduced into the gas, and the results are shown in Figure 4b. When HCl was added into the gas, a momentary increase of Hg^T was observed. This increase may have occurred because the Hg²⁺ formed over the catalyst reacted with HCl to form HgCl₂, which then desorbed into the gas phase, as in reactions 6 and 7. Due to the desorption of oxidized mercury, the active sites on the surface of the catalyst were regenerated, and elemental mercury was adsorbed to the catalyst, which caused the decrease of Hg⁰ shown in Figure 4b.

Figure 4c shows the results of Hg⁰ adsorption over the catalyst in the absence of O₂. After Hg⁰ adsorption equilibrium was reached, no oxidized mercury could be detected (Figure 4c). Next, O₂ gas was introduced, and the concentration of Hg⁰ decreased significantly, likely because the chemisorption of Hg⁰ over the catalyst was improved by the replenishment of oxygen species. We also note that oxidized mercury was generated with the presence of O₂, and the amount increased over time. Though large amounts of oxidized mercury were formed, the concentration of Hg^T decreased until the concentration of Hg⁰ was stable. After that, the Hg^T increased more gradually, and more Hg²⁺ was generated. These results indicate that the oxidation of elemental mercury over the catalyst in the presence of O₂ could proceed through reactions 2–4. Because Figure 4c only shows the initial stage of the chemisorption process, when adsorption equilibrium was not yet reached, the Hg⁰ removal efficiency was much higher. After reaching adsorption

equilibrium, the removal efficiency would likely decrease to approximately 48% (corresponding to the results in Figures 1 and 4d). The catalytic oxidation of Hg⁰ with O₂ and HCl was also monitored by the Tekran mercury analyzer, and the results are shown in Figure 4d. When approximately 370 ng/L Hg⁰ was passed through the catalyst at 350 °C in the presence of O₂, approximately 175 ng/L Hg²⁺ could be detected in the gas after reaching equilibrium, which demonstrates that elemental mercury can be catalytically oxidized by O₂ in the absence of HCl, like the result in Figure 1. This result also proves that the conversion of Hg⁰ could proceed through reactions 2–4. When HCl was introduced into the gas, a momentary significant increase of Hg^T and Hg²⁺ was observed. This could have been caused by the release of Hg²⁺ due to adding of HCl through reactions 5–6. As the oxidized mercury desorbed from the surface of the catalyst into gaseous form, the active sites on the catalyst were regenerated, which would accelerate the chemisorption of Hg⁰ (reactions 2–3), resulting in the decline of Hg⁰ concentration. Because the concentration of Hg⁰ decreased as HCl was added into the gas, the Hg^T also decreased after the initial increase. After the reaction reached equilibrium, the Hg^T began to increase again and finally recovered to its initial level. This indicates that mercury was balanced during the catalytic oxidation reaction.

H₂-TPR. To investigate the redox ability of the catalysts, we tested the temperature program reduction (TPR) by hydrogen for the Ce_{0.6}Zr_{0.4}O₂ and IrO₂/Ce_{0.6}Zr_{0.4}O₂ catalysts. The results are shown in Figure 5. The profile for the Ce_{0.6}Zr_{0.4}O₂ catalyst has a broad reduction peak that begins at 300 °C and is centered at approximately 580 °C. We attribute this peak to the reduction of the Ce⁴⁺ in the Ce–Zr solid solution.^{37,38} A weak peak at 260 °C appears in the profile for the 0.2%IrO₂/ZrO₂ catalyst, which is ascribed to reduction of highly dispersed IrO₂ species.³⁹ Previous studies have shown that it is difficult to reduce ZrO₂ by H₂ at low temperatures, so the reduction peaks at approximately 530 °C over the profile of the 0.2%IrO₂/ZrO₂

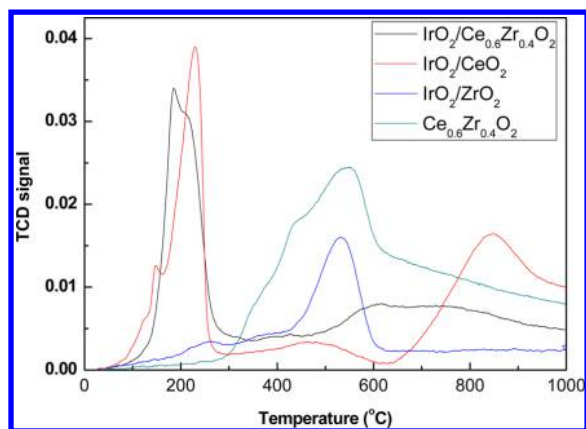


Figure 5. H₂-TPR curves of various catalysts.

catalyst could be caused by the interaction between IrO₂ and ZrO₂ support.⁴⁰ A strong peak is present at approximately 190 °C for the IrO₂/Ce_{0.6}Zr_{0.4}O₂ catalyst, and this is not observed in the profiles of Ce_{0.6}Zr_{0.4}O₂ and IrO₂/ZrO₂. In general, peaks below 200 °C are probably caused by the reduction of crystalline IrO₂ species (large particles), and peaks above 250 °C are caused by the reduction of well-dispersed IrO₂ species.³⁹ However, the peak centered at 190 °C over the IrO₂/Ce_{0.6}Zr_{0.4}O₂ cannot be attributed to the reduction of IrO₂ alone because the content of IrO₂ is only 0.2% and the H₂ consumption amount should be very low (similar to the small peak in the IrO₂/ZrO₂ profile). In addition, the large peak at 580 °C caused by reduction of Ce⁴⁺ in the profile for the IrO₂/Ce_{0.6}Zr_{0.4}O₂ catalyst vanished with the doping of 0.2% IrO₂. To identify the peak, we also show the H₂-TPR curve of IrO₂/CeO₂ in Figure 5, and a similar peak was detected at 210 °C. Therefore, it is reasonable to infer that the strong peak at low temperature (approximately 190 °C) could be explained by the interaction between IrO₂ and Ce–Zr support. Thus, Ir–Ce mixed oxide might exist in the IrO₂/Ce_{0.6}Zr_{0.4}O₂ catalyst, which resulted in an improved oxidation capacity at low temperatures. This would enhance reactions 2–4 over the catalysts and could explain why mercury oxidation in the presence of only O₂ was much more efficient with the addition of IrO₂.

XPS Analysis. To understand the chemical state of the elements on the catalyst surface, we present the XPS spectra of Zr, Ce, and O in Figure S7. Figure S7 shows the core level spectrum of Zr 3d at various binding energies: 182.9 eV for Zr 3d_{5/2} and 184.7 eV for Zr 3d_{3/2}. These peak values are typical of the Zr⁴⁺ in ZrO₂.⁴¹ Complicated Ce 3d XPS spectra for the Ce_{0.6}Zr_{0.4}O₂ and IrO₂/Ce_{0.6}Zr_{0.4}O₂ catalysts are given in Figure S7. The bands labeled u1 and v1 represent the 3d¹⁰4f¹ initial electronic state, corresponding to Ce³⁺ ions, and the peaks labeled as u0, u2, u3, v0, v2, and v3 represent the 3d¹⁰4f⁰ state of the Ce⁴⁺ ions.¹¹ The ratio of Ce³⁺/(Ce³⁺+Ce⁴⁺) can be calculated from the area of these peaks,⁴² and the concentration of Ce³⁺ calculated for the Ce_{0.6}Zr_{0.4}O₂ catalyst was 33.53%. With the doping of 0.2% IrO₂, the percentage of Ce³⁺ ions increased to 40.19%. It has been proposed in many studies that the presence of Ce³⁺ species can create charge imbalance, vacancies, and unsaturated chemical bonds on the surface of the catalysts, which will lead to increase of chemisorbed oxygen on the surface and benefit the catalytic activity.^{11,43} Therefore, the O 1s spectra of various catalysts are also shown in Figure S7. The O 1s peaks can be divided into two peaks corresponding to the lattice oxygen at 529.3–530.0 eV and the chemisorbed

oxygen at 531.3–532 eV.¹¹ Surface chemisorbed oxygen has been reported to be the most active oxygen and plays an important role in oxidation reactions. The concentration of chemisorbed surface oxygen on the Ce_{0.6}Zr_{0.4}O₂ catalyst was 10.13%, and this percentage increased to 66.68% after IrO₂ doping, which supports the idea that the presence of IrO₂ could significantly improve catalytic activity. After Hg⁰ adsorption without O₂ over the IrO₂/Ce_{0.6}Zr_{0.4}O₂ catalyst, the percentage of chemisorbed oxygen decreased to 32.22%, suggesting that the adsorbed Hg⁰ was mainly oxidized by the chemisorbed oxygen species.

The Role of IrO₂ and Another Possible Mechanism. To determine the role of doping with IrO₂ during the Hg⁰ oxidation reaction, we show in Figure S6 the results of the Hg⁰ adsorption experiments over fresh Ce_{0.6}Zr_{0.4}O₂ and HCl-pretreated Ce_{0.6}Zr_{0.4}O₂ catalysts as well as the Hg⁰ adsorption breakthrough curves. The adsorption capacity of Hg⁰ over Ce_{0.6}Zr_{0.4}O₂ was very low, and adsorption equilibration was reached quickly. In contrast, the breakthrough curve over HCl-pretreated Ce_{0.6}Zr_{0.4}O₂ was very different, and the removal efficiency of elemental mercury was as high as 95% for over 400 min. This result is similar to the results in Figure 2, which showed that HCl treatment with or without O₂ could significantly improve the apparent adsorption capacity of Hg⁰ over the catalyst. Because the apparent adsorption capacity of Hg⁰ was improved by HCl treatment whether the catalyst was doped with IrO₂, we infer that doping IrO₂ has no obvious effects on reactions 5–7 (in which HCl functions) in the chemisorption–regeneration mechanism.

Although the H₂-TPR and XPS results indicate that doping with IrO₂ has a synergistic effect with the Ce–Zr carrier and can facilitate the oxidation capacity of the catalyst, the chemisorption process was improved over IrO₂ modified catalyst. However, this result cannot convincingly explain (because of the result in Figure S6) why the addition of 0.2% IrO₂ significantly improved the catalytic efficiency of Hg⁰ in the presence of HCl. As stated previously, the Deacon reaction has been proposed as a mechanism for Hg⁰ oxidation in the presence of HCl over many catalysts, and IrO₂ is an active component for the Deacon reaction. Although Cl₂ has been proven to be not essential for Hg⁰ oxidation, it can act as a marker of catalytic activity because Cl atoms on the catalysts can combine with each other to form Cl₂. Thus, Cl₂ yield over various catalysts was tested to evaluate the Deacon reaction as another possible mechanism. Figure 6 shows that one absorption peak centered at 330 nm is present observed after HCl and O₂ were passed through Ce_{0.6}Zr_{0.4}O₂ catalyst at 350 °C, and the peak can be assigned to Cl₂. With 0.2% IrO₂ doping, the intensity of the adsorption peak increased to over 0.04. Obviously, the preparation method could also affect the production of Cl₂, and the adsorption peak intensity increased to 0.084 over the PVP-promoted IrO₂/Ce_{0.6}Zr_{0.4}O₂ catalyst. The Cl₂ yield capacities decreased in the following sequence: IrO₂/Ce_{0.6}Zr_{0.4}O₂(PVP) > IrO₂/Ce_{0.6}Zr_{0.4}O₂ > Ce_{0.6}Zr_{0.4}O₂. This is the same with catalytic oxidation activity of Hg⁰ over these catalysts in the presence of HCl (Figure 1). Therefore, we infer that Hg⁰ can be oxidized through the Deacon reaction, in which Cl[−] in catalyst or from adsorbed HCl was first oxidized by active oxygen species to atomic chlorine (reaction 9), after which the formed atomic chlorine atoms could combine to generate gaseous Cl₂ if no Hg⁰ was present in gas (reactions 10 and 11). When Hg⁰ existed in the gas and was adsorbed to the surface, the elemental mercury could react with Cl atoms to

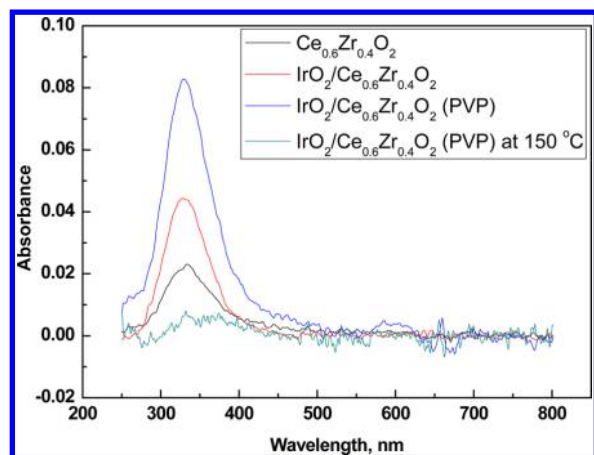
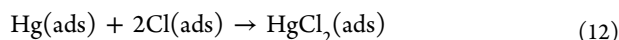
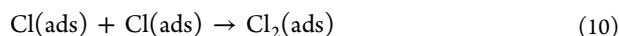
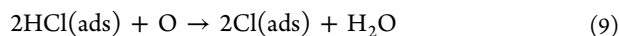


Figure 6. Cl_2 yield over various catalysts. Reaction conditions: 9000 ppm of HCl; O_2 , 4 vol %; N_2 as carrier; flow rate, 40 mL/min; catalyst weight, 60 mg. The space velocity (SV) was approximately $3.04 \times 10^4 \text{ h}^{-1}$. The temperature was $350 \text{ }^\circ\text{C}$.

form HgCl_2 (reaction 12). The overall reaction formula can also be expressed as reaction 8. The Cl_2 yield experiment was also carried out over the catalyst at $150 \text{ }^\circ\text{C}$, and no obvious peak of Cl_2 was detected over the catalyst, which indicates that the Deacon reaction mechanism might only proceed at relatively high temperatures.



According to the results above, there are two possible mechanisms for the catalytic oxidation of Hg^0 over the IrO_2 -modified catalysts (Figure 7). The first mechanism is the chemisorption–regeneration pathway in which Hg^0 is first adsorbed and oxidized by surface chemisorbed oxygen to HgO . The TPR results and XPS spectra showed that doping of IrO_2 significantly increased the percentage of chemisorbed oxygen, such that the oxidation of Hg^0 was enhanced in the presence of IrO_2 . Some previous studies have also proposed that O_2 can be dissociated more easily on IrO_2 , which could increase the replenishment of chemisorbed oxygen and result in superior chemisorption.⁴⁴ The chemisorption process can proceed in the absence of chlorine (lacking both gaseous HCl and Cl^- on the surface), but O_2 was essential. Next, oxidized mercury could

desorb from the surface in the form of HgO (or HgCl_2 in the presence of gaseous HCl). Thus, the active adsorption sites would be regenerated, and the adsorption of Hg^0 could proceed continuously. In the second mechanism, the Deacon reaction, the adsorbed HCl is first oxidized by active oxygen species to active Cl species, and the resulting Cl atoms can combine with each other to form Cl_2 if no Hg^0 is present in the gas. Our results show that doping with IrO_2 can significantly enhance the Cl yield from the reaction. When Hg^0 is adsorbed to the surface of catalyst, it can react with Cl atoms to form HgCl_2 , which can be released into the gas phase. The major difference between these two mechanisms is whether the adsorbed Hg^0 or HCl is first oxidized by active species. Meanwhile, both of the two proposed oxidation processes could be promoted by doping with IrO_2 .

■ ASSOCIATED CONTENT

§ Supporting Information

The Supporting Information is available free of charge on the ACS Publications website at DOI: 10.1021/acs.est.5b05564.

Additional details on the preparation method of the Ce-Zr solid solution. Figures showing the experimental system, The catalytic oxidation of Hg^0 over various catalysts under different condition at $350 \text{ }^\circ\text{C}$; the catalytic oxidation of Hg^0 over $\text{Ce}_{0.6}\text{Zr}_{0.4}\text{O}_2$ with different condition at $350 \text{ }^\circ\text{C}$ and $150 \text{ }^\circ\text{C}$; the catalytic oxidation of Hg^0 over $\text{IrO}_2/\text{Ce}_{0.6}\text{Zr}_{0.4}\text{O}_2$ (PVP) with simulated coal-fired flue gas at 350 and $150 \text{ }^\circ\text{C}$; the adsorption curve over $\text{Ce}_{0.6}\text{Zr}_{0.4}\text{O}_2$; and the XPS spectra of Ce, O, and Zr in various catalysts. (PDF)

■ AUTHOR INFORMATION

Corresponding Author

*Fax: +86 21 54745591; tel: +86 21 54745591; e-mail: nqyan@sjtu.edu.cn.

Notes

The authors declare no competing financial interest.

■ ACKNOWLEDGMENTS

This study was supported by the National Basic Research Program of China (973) under Grant No. 2013CB430005, and the NSFC projects (21277088, 21077073).

■ REFERENCES

- Presto, A. A.; Granite, E. J. Impact of sulfur oxides on mercury capture by activated carbon. *Environ. Sci. Technol.* **2007**, *41* (18), 6579–6584.

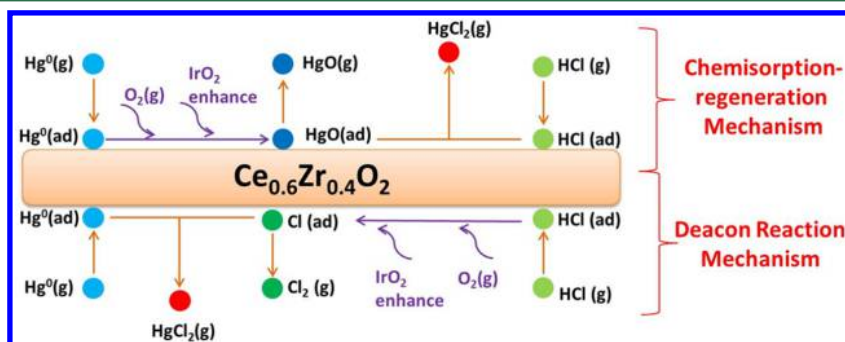


Figure 7. Proposed mechanism of Hg^0 oxidation.

- (2) Presto, A. A.; Granite, E. J.; Karash, A. Further investigation of the impact of sulfur oxides on mercury capture by activated carbon. *Ind. Eng. Chem. Res.* **2007**, *46* (24), 8273–8276.
- (3) Kessler, R. The Minamata Convention on Mercury: a first step toward protecting future generations. *Environ. health. persp.* **2013**, *121* (10), A304.
- (4) Gaffney, J. S.; Marley, N. In-depth review of atmospheric mercury: sources, transformations, and potential sinks. *Inter. J. Nanomed.* **2014**, *9*, 1883–1889.
- (5) Pirrone, N.; Cinnirella, S.; Feng, X.; Finkelman, R.; Friedli, H.; Leaner, J.; Mason, R.; Mukherjee, A.; Stracher, G.; Streets, D.; Telmer, K. Global mercury emissions to the atmosphere from anthropogenic and natural sources. *Atmos. Chem. Phys.* **2010**, *10* (13), 5951–5964.
- (6) Presto, A. A.; Granite, E. J. Survey of catalysts for oxidation of mercury in flue gas. *Environ. Sci. Technol.* **2006**, *40* (18), 5601–5609.
- (7) Wang, Y. J.; Liu, Y.; Wu, Z. B.; Mo, J. S.; Cheng, B. Experimental study on the absorption behaviors of gas phase bivalent mercury in Ca-based wet flue gas desulfurization slurry system. *J. Hazard. Mater.* **2010**, *183* (1–3), 902–907.
- (8) Li, X.; Lee, J. Y.; Heald, S. XAFS characterization of mercury captured on cupric chloride-impregnated sorbents. *Fuel* **2012**, *93* (1), 618–624.
- (9) Wan, Q.; Duan, L.; He, K.; Li, J. Removal of gaseous elemental mercury over a CeO₂–WO₃/TiO₂ nanocomposite in simulated coal-fired flue gas. *Chem. Eng. J.* **2011**, *170* (2), 512–517.
- (10) Liu, Y.; Wang, Y.; Wang, H.; Wu, Z. Catalytic oxidation of gas-phase mercury over Co/TiO₂ catalysts prepared by sol–gel method. *Catal. Commun.* **2011**, *12* (14), 1291–1294.
- (11) Chen, L.; Li, J.; Ge, M. Promotional Effect of Ce-doped V₂O₅–WO₃/TiO₂ with Low Vanadium Loadings for Selective Catalytic Reduction of NO_x by NH₃. *J. Phys. Chem. C* **2009**, *113* (50), 21177–21184.
- (12) Niksa, S.; Fujiwara, N. A predictive mechanism for mercury oxidation on selective catalytic reduction catalysts under coal-derived flue gas. *J. Air Waste Manage. Assoc.* **2005**, *55* (12), 1866–1875.
- (13) Senior, C. L. Oxidation of mercury across selective catalytic reduction catalysts in coal-fired power plants. *J. Air Waste Manage. Assoc.* **2006**, *56* (1), 23–31.
- (14) Yang, S.; Xiong, S.; Liao, Y.; Xiao, X.; Qi, F.; Peng, Y.; Fu, Y.; Shan, W.; Li, J. Mechanism of N₂O Formation during the Low-Temperature Selective Catalytic Reduction of NO with NH₃ over Mn–Fe Spinel. *Environ. Sci. Technol.* **2014**, *48* (17), 10354–10362.
- (15) Galbreath, K. C.; Zygarricke, C. J. Mercury transformations in coal combustion flue gas. *Fuel Process. Technol.* **2000**, *65*, 289–310.
- (16) Li, X.; Liu, Z.; Kim, J.; Lee, J.-Y. Heterogeneous catalytic reaction of elemental mercury vapor over cupric chloride for mercury emissions control. *Appl. Catal., B* **2013**, *132*, 401–407.
- (17) Xu, W.; Wang, H.; Zhou, X.; Zhu, T. CuO/TiO₂ catalysts for gas-phase Hg⁰ catalytic oxidation. *Chem. Eng. J.* **2014**, *243*, 380–385.
- (18) Li, H.; Wu, C.-Y.; Li, Y.; Zhang, J. CeO₂–TiO₂ catalysts for catalytic oxidation of elemental mercury in low-rank coal combustion flue gas. *Environ. Sci. Technol.* **2011**, *45* (17), 7394–7400.
- (19) Over, H.; Schomäcker, R. What Makes a Good Catalyst for the Deacon Process? *ACS Catal.* **2013**, *3* (5), 1034–1046.
- (20) Moser, M.; Mondelli, C.; Amrute, A. P.; Tazawa, A.; Teschner, D.; Schuster, M. E.; Klein-Hoffman, A.; López, N.; Schmidt, T.; Pérez-Ramírez, J. HCl Oxidation on IrO₂-Based Catalysts: From Fundamentals to Scale-Up. *ACS Catal.* **2013**, *3* (12), 2813–2822.
- (21) Ko, J. H.; Park, S. H.; Jeon, J.-K.; Kim, S.-S.; Kim, S. C.; Kim, J. M.; Chang, D.; Park, Y.-K. Low temperature selective catalytic reduction of NO with NH₃ over Mn supported on Ce_{0.65}Zr_{0.35}O₂ prepared by supercritical method: Effect of Mn precursors on NO reduction. *Catal. Today* **2012**, *185* (1), 290–295.
- (22) Wang, Q.; Zhao, B.; Li, G.; Zhou, R. Application of rare earth modified Zr-based ceria-zirconia solid solution in three-way catalyst for automotive emission control. *Environ. Sci. Technol.* **2010**, *44* (10), 3870–3875.
- (23) Si, Z. C.; Weng, D.; Wu, X. D.; Ran, R.; Ma, Z. R. NH₃-SCR activity, hydrothermal stability, sulfur resistance and regeneration of Ce_{0.75}Zr_{0.25}O₂–PO₄³⁻ catalyst. *Catal. Commun.* **2012**, *17*, 146–149.
- (24) Cao, Y.; Gao, Z.; Zhu, J.; Wang, Q.; Huang, Y.; Chiu, C.; Parker, B.; Chu, P.; Pan, W. P. Impacts of halogen additions on mercury oxidation, in a slipstream selective catalyst reduction (SCR), reactor when burning sub-bituminous coal. *Environ. Sci. Technol.* **2008**, *42* (1), 256–261.
- (25) Chen, W.; Ma, Y.; Qu, Z.; Liu, Q.; Huang, W.; Hu, X.; Yan, N. Mechanism of the Selective Catalytic Oxidation of Slip Ammonia over Ru-Modified Ce–Zr Complexes Determined by in Situ Diffuse Reflectance Infrared Fourier Transform Spectroscopy. *Environ. Sci. Technol.* **2014**, *48* (20), 12199–12205.
- (26) Presto, A. A.; Granite, E. J. Noble metal catalysts for mercury oxidation in utility flue gas. *Platinum Met. Rev.* **2008**, *52* (3), 144–154.
- (27) Yu, T.; Zeng, J.; Lim, B.; Xia, Y. Aqueous-Phase Synthesis of Pt/CeO₂ Hybrid Nanostructures and Their Catalytic Properties. *Adv. Mater.* **2010**, *22* (45), 5188–5192.
- (28) Chen, W.; Ma, Y.; Yan, N.; Qu, Z.; Yang, S.; Xie, J.; Guo, Y.; Hu, L.; Jia, J. The co-benefit of elemental mercury oxidation and slip ammonia abatement with SCR-Plus catalysts. *Fuel* **2014**, *133*, 263.
- (29) Yang, S.; Guo, Y.; Yan, N.; Wu, D.; He, H.; Xie, J.; Qu, Z.; Jia, J. Remarkable effect of the incorporation of titanium on the catalytic activity and SO₂ poisoning resistance of magnetic Mn–Fe spinel for elemental mercury capture. *Appl. Catal., B* **2011**, *101* (3), 698–708.
- (30) Xie, J.; Qu, Z.; Yan, N.; Yang, S.; Chen, W.; Hu, L.; Huang, W.; Liu, P. Novel regenerable sorbent based on Zr–Mn binary metal oxides for flue gas mercury retention and recovery. *J. Hazard. Mater.* **2013**, *261*, 206–213.
- (31) Li, H.; Wu, C.-Y.; Li, Y.; Li, L.; Zhao, Y.; Zhang, J. Impact of SO₂ on elemental mercury oxidation over CeO₂–TiO₂ catalyst. *Chem. Eng. J.* **2013**, *219*, 319–326.
- (32) Wan, Q.; Duan, L.; He, K. B.; Li, J. H. Removal of gaseous elemental mercury over a CeO₂–WO₃/TiO₂ nanocomposite in simulated coal-fired flue gas. *Chem. Eng. J.* **2011**, *170* (2–3), 512–517.
- (33) Xie, Y. N.; Li, C. T.; Zhao, L. K.; Zhang, J.; Zeng, G. M.; Zhang, X. N.; Zhang, W.; Tao, S. S. Experimental study on Hg⁰ removal from flue gas over columnar MnO_x–CeO₂/activated coke. *Appl. Surf. Sci.* **2015**, *333*, 59–67.
- (34) Lopez-Anton, M. A.; Yuan, Y.; Perry, R.; Maroto-Valer, M. M. Analysis of mercury species present during coal combustion by thermal desorption. *Fuel* **2010**, *89* (3), 629–634.
- (35) Xu, Y.; Mavrikakis, M. Adsorption and dissociation of O₂ on Ir (111). *J. Chem. Phys.* **2002**, *116* (24), 10846–10853.
- (36) Liu, Y.; Wang, Y. J.; Wang, H. Q.; Wu, Z. B. Catalytic oxidation of gas-phase mercury over Co/TiO₂ catalysts prepared by sol-gel method. *Catal. Commun.* **2011**, *12* (14), 1291–1294.
- (37) Guo, Y.; Lu, G.; Zhang, Z.; Zhang, S.; Qi, Y.; Liu, Y. Preparation of Ce_xZr_{1-x}O₂ (x = 0.75, 0.62) solid solution and its application in Pd-only three-way catalysts. *Catal. Today* **2007**, *126* (3), 296–302.
- (38) Zhi Min, L.; Jian Li, W.; Jun Bo, Z.; Yao Qiang, C.; Sheng Hui, Y.; Mao Chu, G. Catalytic combustion of toluene over platinum supported on Ce–Zr–O solid solution modified by Y and Mn. *J. Hazard. Mater.* **2007**, *149* (3), 742–746.
- (39) Hong, X.; Li, B.; Wang, Y. J.; Lu, J. Q.; Hu, G. S.; Luo, M. F. Stable Ir/SiO₂ catalyst for selective hydrogenation of crotonaldehyde. *Appl. Surf. Sci.* **2013**, *270*, 388–394.
- (40) Xie, J. K.; Qu, Z.; Yan, N. Q.; Yang, S. J.; Chen, W. M.; Hu, L. G.; Huang, W. J.; Liu, P. Novel regenerable sorbent based on Zr–Mn binary metal oxides for flue gas mercury retention and recovery. *J. Hazard. Mater.* **2013**, *261*, 206–213.
- (41) Reddy, B. M.; Chowdhury, B.; Smirniotis, P. G. An XPS study of the dispersion of MoO₃ on TiO₂–ZrO₂, TiO₂–SiO₂, TiO₂–Al₂O₃, SiO₂–ZrO₂, and SiO₂–TiO₂–ZrO₂ mixed oxides. *Appl. Catal., A* **2001**, *211* (1), 19–30.
- (42) Prusty, D.; Pathak, A.; Mukherjee, M.; Mukherjee, B.; Chowdhury, A. TEM and XPS studies on the faceted nanocrystals of Ce_{0.8}Zr_{0.2}O₂. *Mater. Charact.* **2015**, *100*, 31–35.

- (43) Yang, S. X.; Zhu, W. P.; Jiang, Z. P.; Chen, Z. X.; Wang, J. B. The surface properties and the activities in catalytic wet air oxidation over CeO₂-TiO₂ catalysts. *Appl. Surf. Sci.* **2006**, *252* (24), 8499–8505.
- (44) Wang, H.; Schneider, W. F.; Schmidt, D. Intermediates and spectators in O₂ dissociation at the RuO₂ (110) surface. *J. Phys. Chem. C* **2009**, *113* (34), 15266–15273.